

A mathematical model for growth of solid tumors and combination therapy with an application to colorectal cancer

Valeria De Mattei[†], Franco Flandoli[†], Marta Leocata[†], Maria Cristina Polito[†], and Cristiano Ricci[‡]

[†]Department of Mathematics, University of Pisa

[‡]Department of Mathematics and Computer Science, University of Florence

April 9, 2018

Abstract

We present a mathematical model, based on ordinary differential equations, for the evolution of solid tumors and their response to treatment. Specifically the effects of a cytotoxic agent and a monoclonal antibody are included as control term in the equations. The variables considered here are: the number of cancerous cells sensitive to chemotherapy, the number of cancerous cells resistant to chemotherapy, the degree of angiogenesis and the average intensity of VEGF. The rules that govern the quantities mentioned above are based on a geometrical argument: we approximate the tumor mass as a sphere and thus derive basic formulae for the normoxic cells and for VEGF production. The monoclonal antibody acts on VEGF and thus has influence to the global degree of angiogenesis. Numerical estimates on some of the parameters are performed in order to match the main landmark in tumor progression and reaction to treatment in the specific case of colorectal cancer.

1 Introduction

Mathematical oncology promises to be a powerful tool to study cancer progression. Differential equations models for various quantities, including a spatial structure or not, have been developed with the specific purpose of analyzing the change in tumor size over time. In addition, mathematical models are also helpful to understand the long term dynamics of tumor growth as well as to test biological hypothesis or to evaluate different treatment options. Various technique for quantitative estimates are applied in order to match quantitative values proper of this disease: this is possible after a rigorous calibration of such models using clinical or experimental data.

Several mathematical models of tumor growth based on ordinary differential equations have been proposed in literature. The core of these models is the presence of two equations for the number of cells and the carrying capacity, that is the level of angiogenesis. The models can reproduce the main features of tumor growth, see for instance [6], [23], where tumor growth is gompertzian, or [44], with a modification of gompertzian growth, or [14], where the tumor growth is logistic. Some of these models based on ODE do not omit the spatial structure completely: some of them apply a spherical approximation of the tumor mass (multicellular tumor spheroids) and prescribe a growth rule based on such approximation, see [33] for an example.

VEGF has already been introduced in previous models: in [18], [27], [39] molecularly detailed models of VEGF have been studied; [1] and [3] introduce ODEs models involving the number of cells, angiogenesis and growth factors. In literature several models involving cytotoxic and antiangiogenic therapies can be found: see [6], where combination between cytotoxic and antiangiogenic therapies is being optimized, [5], where the cytotoxic and antiangiogenic drugs are combined with surgery, [32] and [34], again comparing cytotoxic and antiangiogenic agents, and [2], where a model involving antiangiogenic therapy is studied. Moreover, models which involve cytotoxic agents impose a complex argument: birth and evolution of drug resistance cells, widely studied in [11][15][31] [43][48].

Inspired by previous works we aim to formulate a mathematical model that is able to match the main landmarks in tumor development in the growth phase as well as the response to specific treatment, with a reasonable level of approximation. Summarizing, the general aims of this paper are the following: (1) we want to develop a model to reproduce qualitative aspects of the growth, specifically the transition between the exponential growth in the beginning and a slower regimen when the number of cells increase, trying to partially restore the exponential growth after the angiogenesis takes place. (2) We would like to specialize our model to a concrete case (colorectal cancer) and calibrate the parameters in order to match quantitative values proper of this disease. (3) Referring to the previous point, we want to embed in our model a combination therapy in order to compare the results obtained with those coming from clinical trials. Specifically, we have in mind to include the action of a cytotoxic agent, directly on the number of cells, as well as the action of an antiangiogenic agent on the VEGF variable. We also plan to introduce drug-resistant cells into the system to take into account the deterioration of chemotherapy efficacy.

The paper is organized as follow. The mathematical model is presented in section 2. Section 3 is entirely devoted to the choices for the parameters, whose calibration was performed in the specific case of colorectal cancer, while in section 4 we present the numerical results concerning size and TTP (time to progression) in a specific treatment regimen. Finally in section 5, a brief conclusion is given.

2 The mathematical model

The general rationale of our model construction has been to use a very small number of variables, with a clear biophysical meaning, simple but still preserving general main mechanisms of cancer growth. We neglect details of the spatial structure and thus do not consider the position of cancer cells and the space-dependence of VEGF concentration and vascularization. We consider the following variables:

- N_t^{sens} = number of drug-sensitive cells;
- N_t^{res} = number of drug-resistant cells;
- V_t = intensity of VEGF field (space average);
- A_t = level of vascularization due to angiogenesis (space average).

For convenience we introduce also the total number of cells:

- $N_t = N_t^{sens} + N_t^{norm}$.

In order to include the effect of a cytotoxic agent (5-FU) we divide the population of cancerous cells into two subpopulations: here N_t^{sens} represents the number of cells sensitive to chemotherapy and N_t^{res} the number of drug-resistant cells. Although the complexity of drug-resistance phenomenon, we assumed for simplicity the resistance as a binary property. To describe the dynamic of the two populations we follow the classical approach of distinguishing the proliferative behavior according to oxygen availability. Thus we divide each population of cells into two subclasses: normoxic (hence potentially proliferating) and hypoxic cells, denoted by $N_t^{i,norm}$ and $N_t^{i,hypo}$ respectively.

Let us now describe the differential equations satisfied by the previous quantities:

$$\frac{d}{dt}N_t^{sens} = (1 - p) \cdot (1 - u_t^{FU}) \cdot \lambda N_t^{sens,norm} - \mu N_t^{sens} \quad (1)$$

$$\frac{d}{dt}N_t^{res} = p \cdot (1 - u_t^{FU}) \cdot \lambda N_t^{sens,norm} + \lambda N_t^{res,norm} - \mu N_t^{res} \quad (2)$$

$$\frac{d}{dt}V_t = \left(C_{hypo \rightarrow V} \left(\frac{N_t^{hypo}}{N_t} \right)^{2/3} - C_{A,V} A_t - C_{beva \rightarrow V} u_t^{beva} \right) V_t (1 - V_t) \quad (3)$$

$$\frac{d}{dt}A_t = 1_{V_t > V_0} C_{V \rightarrow A} (V_t - V_0) (A_t + A_0) (1 - A_t) - 2A_t^{k_A} 1_{V_t \leq V_0} \quad (4)$$

where

$$N_t^{i,hypo} = (1 - A_t) N_t^i \left(1 - \frac{1}{1 + (N_t^i)^{1/3} / 2\eta_i} \right)^3 \quad (5)$$

and u_t^{FU} and u_t^{beva} describes the tissue concentration of the cytotoxic agent and of the monoclonal antibody respectively (more details in section 4.2).

2.1 On the geometrical configuration of the hypoxic and normoxic cells

Let us now introduce the spherical approximation that we have used to describe the variable fraction of the normoxic (resp. hypoxic) cells over the total number of cells. We assume that there are two classes of normoxic cells: those near the boundary of the tumor mass, and those not near the boundary but reached by the new vascular network produced by the angiogenic cascade. In order to have a simple formula for the boundary of the tumor, we assume it has a spherical shape - this is true only approximately, for various reasons, including the complex geometry of real tissues and the rugosity of the surface, but we cannot include these factors unless we go back to space-dependent models. Let δ be the thickness of the proliferating boundary and let R and r be the radius of the tumor mass and of a single tumor cell respectively. By a simple calculation we have

$$N_{boundary}^{norm} = N \left(1 - \left(1 - \frac{\delta}{R} \right)^3 \right)$$

Let us consider two extreme regimes regarding tumor size. When the tumor is very small, $\delta = R$. When the tumor is very large, we assume δ stabilizes to a certain number η of cell diameters, hence $\delta = 2\eta r_{cell}$. Therefore

$$\frac{\delta}{R} = \begin{cases} 1 & \text{when } N \text{ is small} \\ 2\eta/N^{1/3} & \text{when } N \text{ is large} \end{cases} .$$

A simple function which interpolates these two extremes is

$$\frac{\delta}{R} = f(N, \eta) = \frac{1}{1 + N^{1/3}/2\eta} .$$

Thus, we arrive to the formula:

$$N_{boundary}^{norm} = N \left(1 - \left(1 - \frac{1}{1 + N^{1/3}/2\eta} \right)^3 \right) .$$

The contribution coming from those cells, in the complementary of the boundary layer, which are sufficiently angiogenized to be considered as normoxic, is given by

$$N_{angio}^{norm} = A \cdot N \left(1 - \frac{1}{1 + (N)^{1/3}/2\eta} \right)^3 ,$$

where A_t is the average level of vascularization defined above. The hypoxic cells are simply obtained by difference.

2.2 Growth dynamics of sensitive and resistant cells

The reason of deterioration of therapy we take into account is the presence of drug-resistant mutations. We shall rewrite equation (1) and (2) using vector notation:

$$\frac{d}{dt}N_t = \lambda U P^t N_t^{norm} - \mu N_t \quad (6)$$

where

$$N_t = \begin{pmatrix} N_t^{sens} \\ N_t^{res} \end{pmatrix}, \quad N_t^{norm} = \begin{pmatrix} N_t^{sens,norm} \\ N_t^{res,norm} \end{pmatrix}, \quad P = \begin{bmatrix} 1-p & p \\ 0 & 1 \end{bmatrix}, \quad U = \begin{bmatrix} 1-u_t^{FU} & 0 \\ 0 & 1 \end{bmatrix}.$$

We simplify and prescribe that each cancer cell, during a duplication, has a probability p of developing a drug-resistant mutation. The mechanism of mutation is like a change of species. Following this general rationale we summarized this phenomenon by the transition matrix P of a Markov chain. A precise rule of growth of the two subpopulations N_t^{sens} , N_t^{res} would be quite intricate and depend on the relative geometry. Indeed, the approximation of a spherical shape cannot work simultaneously for both, since they are interlaced. Let us distinguish before and after treatment. Before treatment, $N_t^{sens} \gg N_t^{res}$, hence the sphere approximation for drug-sensitive is reasonable. But drug-resistant cells are distributed, inside the tumor mass, in a quite complex way. Somewhere we expect to see kernels of drug-resistant cells due to a first mutated cell together with its descendants; however, this kernel cannot proliferate indefinitely as the global tumor mass because it is partially or completely absorbed into the deeper, hypoxic. In order to “close” our equations, we conjecture that the proliferating boundary of the drug-resistant cells is thinner than the case of sensitive cells. For this reason, and for the sake of simplicity, we use the same spherical approximation even for the resistant cells but we take $\eta_{res} < \eta_{sens}$. After treatment, the approximation as two separate spheres becomes more reasonable, since mutated kernels of cells may remain isolated by the loss of surrounding non-mutated cells and, again to simplify, we assume that the drug-resistant mass is dominated by the largest kernel of mutated cells, so the approximation as a single sphere is not too distant from reality. In this case we thus take $\eta_{res} = \eta_{sens}$.

We point out that equation (6) contains a small inaccuracy: during treatment sensitive cells are affected by chemotherapy while resistant cells are not. In this phase the control term $1 - u_t^{FU}$ is negative and causes a decrease in the number of sensitive cells: this decrease is slightly altered due to the fact that $N_t^{sens,norm}$ is scaled by the term $(1-p)$ coming from the matrix P . In practise this inaccuracy will be numerically negligible given that average values of p will range from 10^{-6} to 10^{-4} and thus $(1-p) \sim 1$.

2.3 The 2/3 formula for VEGF and the angiogenesis (de)generation

The VEGF field is produced by hypoxic cells and absorbed by endothelial cells. The factor $V_t(1 - V_t)$ in equation (3) has the role to restrict V_t in $(0, 1)$, where the choice of 1 as

maximal value of V_t is conventional. The term $-C_{A,V}A_t$ is the natural one to describe absorption by endothelial cells - moreover, it will play a very marginal role in the sequel.

The 2/3 rule for VEGF production by hypoxic cells is justified by the argument that follows. Consider the sphere of hypoxic cells as it were a uniformly “charged” sphere of radius $R - \delta$: it induces the electric field

$$E(r) = \frac{C(R - \delta)^3}{r^2},$$

for a suitable constant C . The potential on the boundary of the sphere is

$$V(R) = C(R - \delta)^2.$$

This is the work done by the electric field to move a point charge from infinity to the boundary of the sphere. In analogy, we think to VEGF as the work needed to move blood vessels from an infinite distance to the sphere of hypoxic cells. Thus VEGF would have the form

$$V_t = C(R_t - \delta_t)^2 = \tilde{C}(N_t^{hypox})^{2/3}$$

with a new constant \tilde{C} .

The equation (4) describes the growth of vasculature by the term

$$1_{V_t > V_0} C_{V \rightarrow A} (V_t - V_0) (A_t + A_0) (1 - A_t),$$

while the second term

$$-2A_t^{k_A} 1_{V_t \leq V_0}$$

concerns the regression due to monoclonal antibody. The bio-mechanical rule of regression is different from the one of accretion. Indeed, when regression occurs, the more recent capillaries are still poor in structure - e.g. not so covered by pericytes - and are easily destroyed, in a short time (of the order of a week) compared with the long times of the overall process (of the order of many years). On the contrary, the less recent angiogenic vasculature has already reached a certain level of stability and thus it regresses much slowly. We have devised, with some degree of approximation and of ad-hoc numerical trials, the above law for the regression.

The term A_0 has been added because for values of A_t very close to zero - even equal to zero - the growth $\frac{d}{dt}A_t$ is not infinitesimal, but finite non zero, due to the presence of the pre-existing vasculature.

The term V_0 corresponds to the fact that angiogenesis requires some degree of concentration of VEGF. Below such threshold no angiogenesis occurs; or more precisely, a regression takes place.

Parameters	Meaning	Value	Source
λ	growth rate due to cell proliferation	0.05	[8][17][43][49]
μ	decay rate due to cell loss	0.002	[8][17][43][49]
η_{sens}	thickness of proliferating boundary of drug-sensitive cells	15	[50]
η_{res}	thickness of proliferating boundary of drug-resistant cells	$\frac{\eta_{sens}}{1.2}$	estimated/simulations
$C_{hypo \rightarrow V}$	VEGF production rate from hypoxic cells	0.08	estimated/simulations
$C_{A,V}$	absorption rate of VEGF from vasculature	0.01	estimated/simulations
$C_{V \rightarrow A}$	reaction rate of angiogenesis to VEGF	0.006	estimated/simulations
A_0	preexistence level of vascularization	0.2	estimated/simulations
k_A	angiogenesis regression rate	10	estimated/simulations
V_0	VEGF threshold for angiogenesis progression	0.2	estimated/simulations
p	probability of drug resistant mutation per cell per duplication	10^{-5}	[11][15][31] [43][48]
N_{start}	number of cells when therapy starts	10^9	[35][51]
N_{FU}	number of days of action of 5-FU (1 to 7)	6	[41]
C_{FU}	intensity of 5-FU action	20	estimated/simulations
N_{beva}	number of days of action of BV5 (1 to 14)	12	[20][37]
$C_{beva \rightarrow V}$	inhibition rate of bevacizumab on VEGF	1	estimated/simulations

Table 1: Parameters of the model. Parameters with no source have been estimated indirectly, refer to section 4.2.

3 Parameters

This section specializes our model to the case of colorectal cancer. As one can appreciate from table 1, some values of parameters are available in literature while others, harder to measure, are estimated experimentally. The first class will be discussed here, while the others are argued in section 4.2.

We based our approximation of (λ, μ) on the estimate of doubling time of colorectal cancer. From the literature (see for instance [17] [8], [43], [49]) DT of the order of 60-180 days seems possible (also less and more). Some authors (see [45], [7]) claim that periods of the order of 8 years could be reasonable estimates of the time needed to reach 10^9 cells and this result is not incompatible with the previous estimates of DT, up to some degree of approximation. We have chosen to impose roughly 8 years to our model to reach 10^9 cells and we have computed an average DT of the order of 100 days, where by average we mean that we take into account the changes of speed of growth that our model has, we compute at every time the instantaneous doubling time and we average it (fig. 1). Obviously there

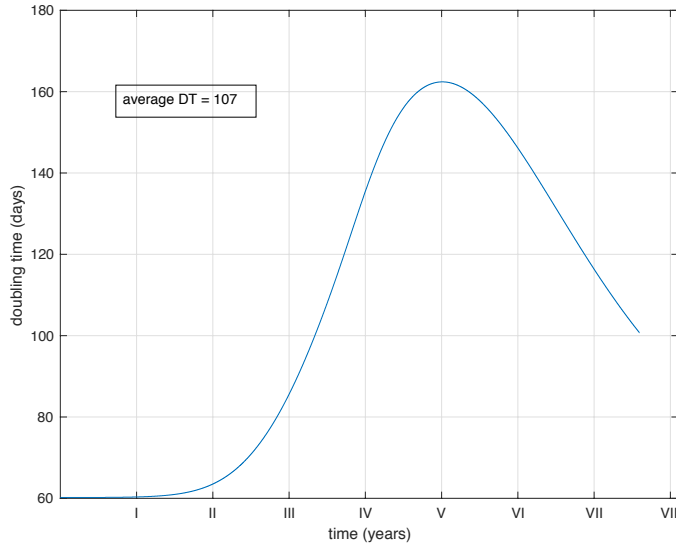


Figure 1: Instantaneous doubling time (DT) as it varies over the whole period. The average is 107, coherent with the literature.

are several choices of parameters which produce these results. We choose as a standard the values in table 1.

The number of cells when therapy starts is obtained by translating available statistics about the volume which around tumors become detectable ($\sim 1cm^3$), see for instance [35] [51].

For what concerns the thickness of proliferating boundary η_{sens} , we obtain the range 5 – 30 through two different arguments. The first one is given by experimental estimates about the distance from a capillary at which cells start to be hypoxic or even necrotic; see a collection of results in [50], figure 13.27 and references therein. These estimates range between 60 and 110 μm , namely less than 10 cells. However, the external proliferating layer is exposed to a much richer amount of oxygen and nutrients than a packed tumor around a capillary. Thus, the previous estimates should be corrected in the increasing direction. Another argument comes from the observation that tumors with radius of size around 1mm are usually avascular, hence for them the proportion α of proliferating boundary with respect to the total is not small. Let us see that values of α of the order 0.25, 0.50, 0.74 give rise to estimates of η_{sens} again of the order of 10. We assume as above that the cell radius is $6\mu m = 6 \cdot 10^{-3}mm$. Similarly to the computation of the section 2.1 we assume to have a spherical tumor of radius R and an external proliferating layer of thickness δ ; hence, in mm , $\delta = 2 \cdot 6 \cdot 10^{-3}\eta_{sens}$. We want to estimate δ , and therefore $\eta_{sens} = 10^3\delta/12$.

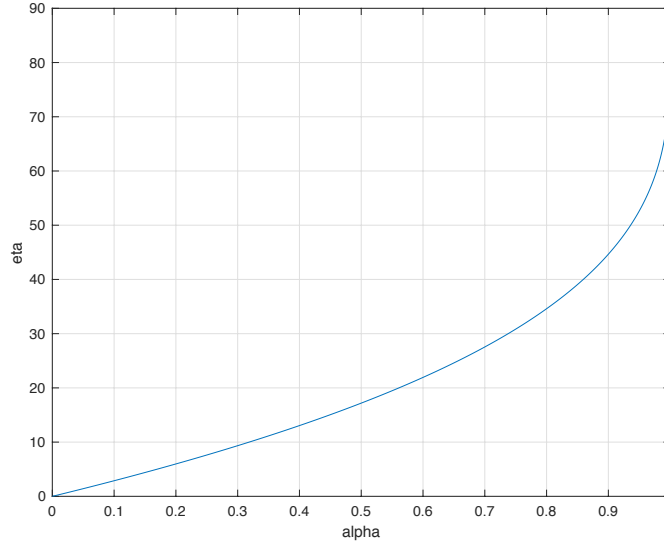


Figure 2: Size of η as a function of α , see text.

The number α is the ratio between the two volumes, hence

$$\alpha = \frac{R^3 - (R - \delta)^3}{R^3} = 1 - (1 - \delta)^3$$

where we have used $R = 1$. Hence

$$\eta_{sens} = \frac{10^3 (1 - \sqrt[3]{1 - \alpha})}{12}.$$

We see from figure 2 that reasonable values are around 10-30; mixing with [50] we choose $\eta = 15$.

The value of p is a very delicate issue, see [15]: it derives from the assumption that the mechanism of mutation is a binary random variable. Our reference value has been 10^{-5} and the range under randomization has been between 10^{-4} and 10^{-6} : we obtained this values by numerical simulations comparing our results with the clinical about TTP found in [29], more details in section 4.2. In support of these values let us quote for instance [48], [21] (page 3650), [31] (section 5.3), [11]. The long time between cell divisions of colorectal cancer cells may be a factor of increase of p , see [19].

The parameters $N_{FU}, C_{FU}, N_{beva}, C_{beva \rightarrow V}$ are included in the control functions u_t^{FU}, u_t^{beva} . Concerning 5-FU, its half-life in plasma is very short, of the order of 10-20 minutes, but in tissues occupied by cancer cells appreciable levels are measured for days, see [41] (in particular figure 1). Concerning BV5, it seems it remains active for a long period, see for

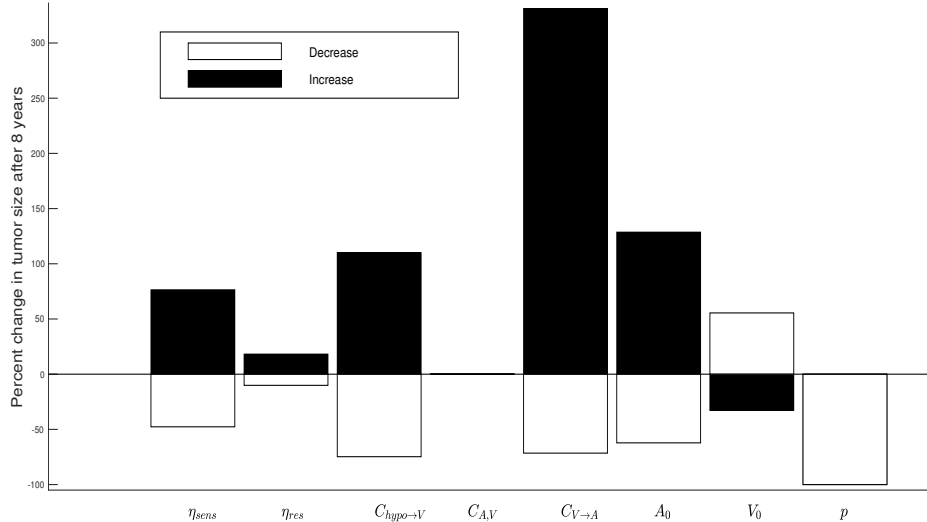


Figure 3: Sensitivity analysis: parameters changed vs percentage change in tumor size after 8 years of growth. Parameters are changed of 50% from table 1, except p , which is altered from 10^{-6} to 10^{-4} .

instance [20][37], thus we take $N_{beva} = 12$. The study of parameters, whose values are not known in literature, represents one of the most difficult point of our work: the idea was to search for the range of admissible values through numerical simulations. Fixing some constraints we have studied the reasonable value of parameters. As largely explained in the following section, we have in mind two kind of constraints: the first class consists of universal characteristics of tumor evolution while the second consists of specifics of colorectal cancer.

4 Numerical Simulations

In this section we propose two different approaches to investigate and validate the model. In the first section we show the biological events caught by our model, while in the second, focused on therapy, we try to compare our result with clinical data proposed in [29].

4.1 General shape of growth

By observing figure 5 we can appreciate the general shape of the growth curve over a large time interval (roughly ten years). When the tumor is small we have $N_{boundary}^{norm} \sim N$, hence in the first segment of the curve the growth is purely exponential. When the tumor is

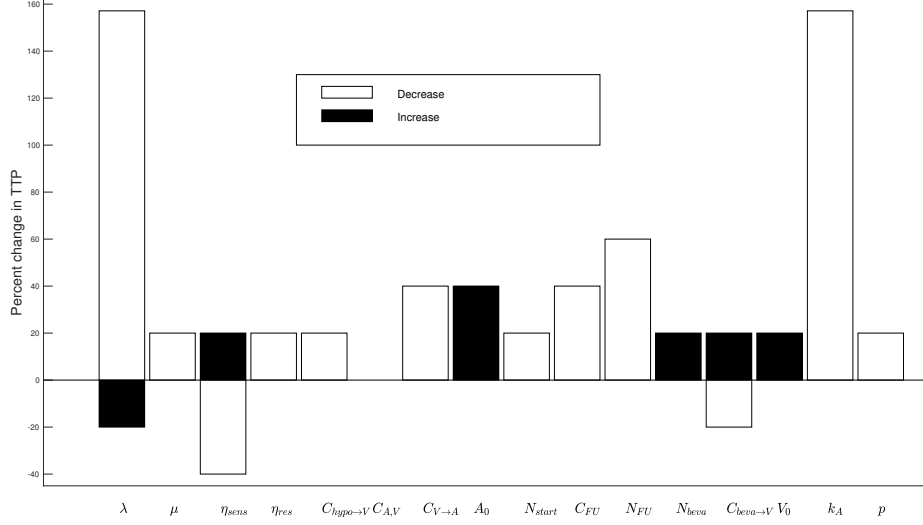


Figure 4: Sensitivity analysis: parameters changed vs percentage change in TTP after treatment (see section 4.2). Parameters are changed of 50% from table 1, except p and N_{start} , which are altered from 10^{-6} to 10^{-4} and from 10^8 to 10^{10} respectively.

larger, namely when $N^{1/3}/\eta \gg 1$, we have

$$N_{layer}^{norm} \sim N \left(1 - \left(1 - \frac{2\eta}{N^{1/3}} \right)^3 \right) \sim 3N \frac{2\eta}{N^{1/3}} = 6\eta N^{2/3}.$$

The 2/3 law often appears in the literature, see for instance [46] and the references therein. Later on, thanks to the angiogenic contribution, we restore the exponential growth rate: in fact when N is large

$$N \left(1 - \frac{1}{1 + N^{1/3}/\eta} \right)^3 \sim N.$$

Comparing the solution of the system (1)-(4) with a classical Gompertz model, characterized by only two phases, it is possible to distinguish a third phase where the exponential rate is restored by angiogenesis.

Keeping in mind the focus on colorectal cancer, we direct our attention to the numerical values proper of this disease:

- roughly 8 years to reach 10^9 cells $\sim 1cm^3$;
- angiogenesis starting between 10^6 and $2 \cdot 10^6$.

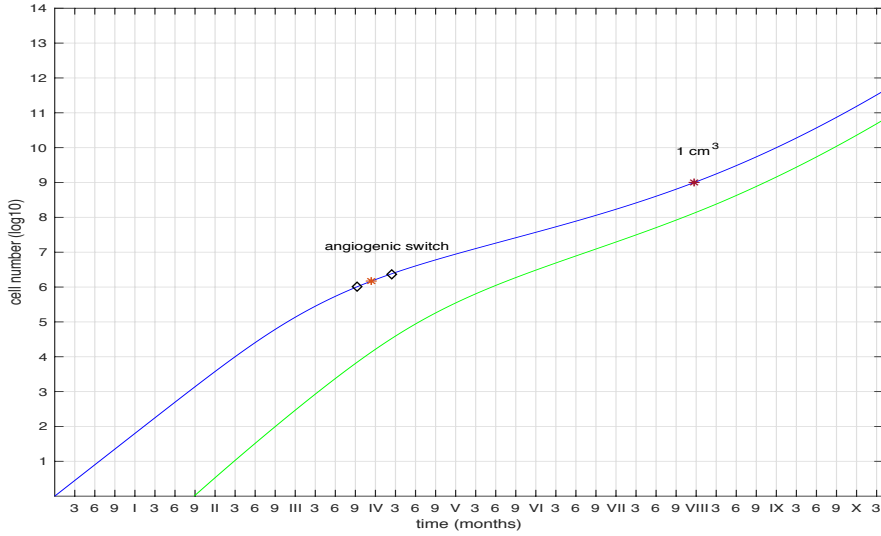


Figure 5: Simulation without therapy. Diamonds denote the range $10^6 - 2 \cdot 10^6$ where angiogenesis is expected to start and the first red star is that initial time. The second red star is when 10^9 cells are reached which should be close to 8 years. Blue line denotes total number of cancer cells, green line those having a drug resistant mutation. Concerning parameters, their value for this simulation is given in table 1 of sections 3.

The first landmark of 1cm^3 has already been argued in section 3. Concerning the starting of the angiogenic cascade, 1mm^3 is a typical order of magnitude of the largest avascular tumors. Around $1 - 2\text{mm}^3$ the angiogenic cascade starts, see [36]. This translates to the range $10^6 - 2 \cdot 10^6$. With these values in mind we have chosen the parameters $C_{\text{hypo} \rightarrow V}, C_{A,V}, C_{V \rightarrow A}, A_0$ in order to reproduce these specific events. Obviously there are several choices of parameters which produce these results (see figure 5). We choose as standard the values in table 1. To deepen how the just mentioned parameters influence the model, we propose the analysis of sensitivity in figure 3. From this analysis one can appreciate the fact that, increasing (resp. decreasing) of 50% parameters which calibrate rate of angiogenesis development ($C_{\text{hypo} \rightarrow V}, C_{V \rightarrow A}$), implies a relevant increase (resp. decrease) of tumor size. The same linear effect arises from the parameters that influence the rate of proliferation for sensitive and resistant cells ($\eta_{\text{sens}}, \eta_{\text{res}}$). Given the strict correlation between (λ, μ) they have not been tested in this phase. In conclusion, the shape of growth curve seems to be very stable with respect to parameters: their alteration entails the maintenance of the three phases, above mentioned.

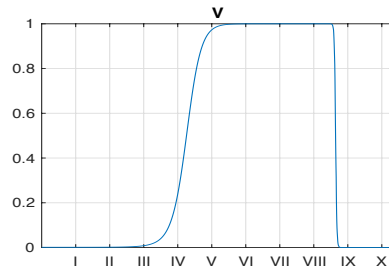
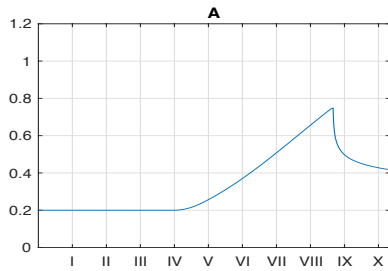
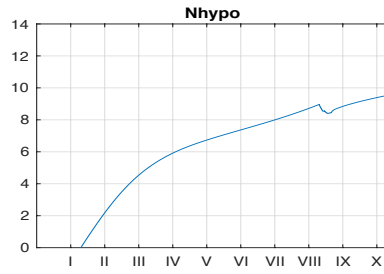
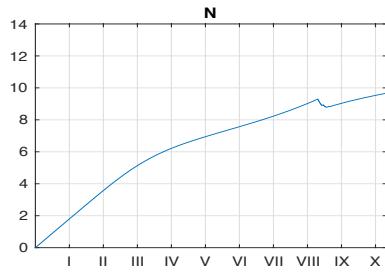
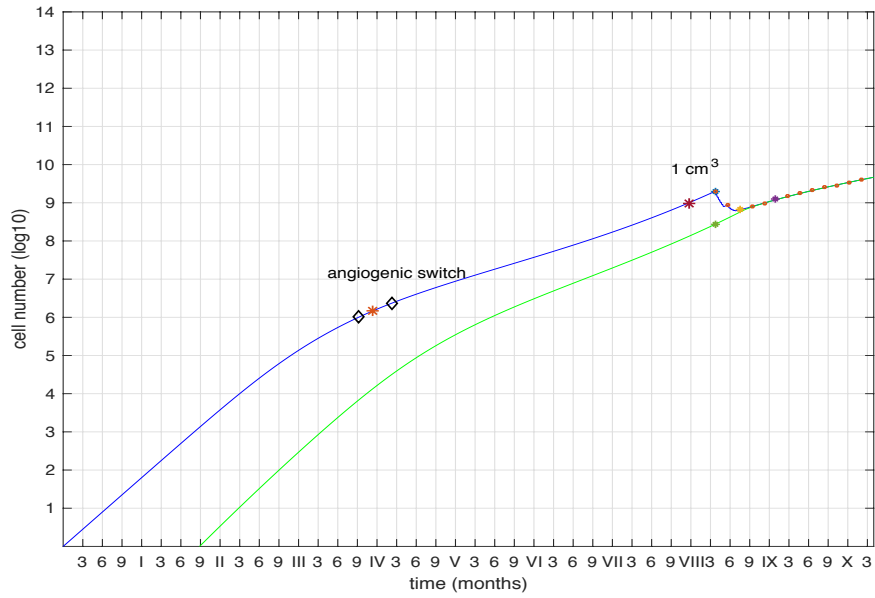


Figure 6: Simulation with therapy, 5-FU plus BV5. Circles denote times of assessment of tumor size. Small subgraphs show the behavior of total number of cells, hypoxic cells, degree of angiogenesis and density of VEGF.

4.2 Connections with clinical data

In this section, we follow a second type of validation mechanism for the model: we adapt the model to a specific case and we try to compare the results obtained through simulations with those found in literature. In clinical trials, when tumor progression takes place, the first line therapy is interrupted and patients could receive any second line treatment, which however may vary and be thus less suitable for a mathematical modeling. Hence, we limit ourselves to a model of the 5-FU or 5-FU + BV5 regimen during the first-line therapy and we measure TTP. Our model is not able to capture the spatial structure of the tumor, so we limit our measurement of TTP on a single lesion of the colorectal cancer. According to [29] and RECIST criteria, we start from time t_0 when therapy begins and register the number of cells every 8 weeks, namely at the end of each cycle; hence, using the spherical approximation, we convert number of cells into lesion diameter and we compute the first measurement with an increase of at least 20 percent from the minimum registered. Following [29], we investigate the case when patients are initially treated by 12 cycles of 5-FU (plus folinic acid), each cycle being of 8 weeks with 5-FU administrated at the beginning of each one of the first 6 weeks of a cycle. We compare this regimen with the one based on 5-FU (and folinic acid) plus bevacizumab. This monoclonal antibody is given once every two weeks - also the last two weeks of the cycle. The particular regimen bevacizumab 5 mg/kg every 2 weeks will be denoted by BV5 and we refer only to it when experimental data are quoted. We remind that u_t^{FU} and u_t^{beva} denote the control functions corresponding to 5-FU and bevacizumab respectively, functions which are equal to zero when 5-FU and BV5 are not present in the tissue. To be precise, they describe the concentration of 5-FU and BV5 in the tumor tissue. Two possible misunderstandings should be avoided: i) the controls u_t^{FU} and u_t^{beva} are not understood as the actions of drug administration, which are short in time like in the case of 5-FU in bolus; ii) they correspond to drug concentration in the tumor tissue, not in plasma. We prescribe that the first administration of 5-FU (+BV5) takes place when the total number of cells reaches the value of N_{start} . Concerning 5-FU, we keep into account two facts: i) cell kill by chemotherapy is faster than proliferation; ii) the concentration of 5-FU in the tissue decays exponentially in time. Using the following expression:

$$u_t^{FU} = (1 + C_{FU}) \exp\left(-\frac{\log(1 + C_{FU})}{N_{FU}} t\right).$$

we obtain that at the beginning of the week, when 5-FU is given in bolus, the rate is equal to

$$\lambda(1 - u_0^{FU}) = \lambda C_{FU}.$$

Hence the constant C_{FU} acts as a multiplier of intensity of cell kill with respect to cell proliferation. A typical value we use is $C_{FU} = 20$. The expression inside the exponential has the following motivation: at time $t = N_{FU}$, we have $u_t^{FU} = 1$, hence the rate at that time is $\lambda(1 - u_{N_{FU}}^{FU}) = 0$. In other words, prescribing the number N_{FU} of days of action

of 5-FU, we prescribe that cell loss occurs until time N_{FU} , in an exponentially decreasing manner; and afterwards proliferation restarts but not immediately with full rate λ , just with rate $\lambda(1 - u_t^{FU})$ which is asymptotic to λ for large times.

Concerning bevacizumab, it is given once every two weeks in each cycle. In the periods of no treatment, $u_t^{beva} = 0$. Under treatment, we impose that its half-life is N_{BV} , hence the form is

$$u_t^{beva} = \exp\left(-\frac{\log 2}{N_{BV}}t\right).$$

In figure 6 it is shown the simulation of the therapy, including bevacizumab. Two of nine parameters whose values are not available in literature are included in the control functions, namely C_{FU} , $C_{beva \rightarrow V}$. In figure 7 it is shown the time segment where the therapy is active. According to clinical results shown in [29], our model catches the relevant significance of addition of BV5 to the therapy: in this case TTP is increased from 7.5 months to 9.3 months (in [29] PFS increases from 7.3 to 9.2). As explained in section 3, some of the parameters whose values are missing, are estimated in an indirect way: we estimated these parameters, in order to obtain reasonable results of TTP (see fig 4 pag. in [29]) and maintaining at the same time the biological constraints described in the previous section. In figure 4 we can appreciate how parameters influence effectiveness of the therapies. The rate of angiogenesis regression, as well as the reaction rate of angiogenesis to VEGF, affects inversely the efficacy of therapy, in particular of bevacizumab. Moreover parameters linked to chemoresistant cells, η_{res}, p , act inversely on TTP, while the thickness of proliferating boundary acts proportionally, according to the fact that chemotherapy kills only proliferating cells. Although altering (λ, μ) will break the specific constraints imposed in subsection 4.1, we include them into the analysis of sensitivity in order to show how growth rate influences TTP.

5 Conclusion

We have devised a mathematical model that governs cancer growth, specifically in the case of solid tumors, and includes the action of a cytotoxic agent and of a monoclonal antibody as control terms. The equations considered here have been proved to be suitable to the case of colorectal cancer. Further investigation is required to claim their applicability to other kind of solid tumors, provided that the spherical approximation is reasonable. The action of the control functions could be used in a variety of context where the effect of such treatment is required, but again, this will require additional effort to be established.

The model is formulated as a system of ordinary differential equations that describe the total number of cells, both sensible and resistant to the cytotoxic agent, the intensity of VEGF field and the level of vascularization due to angiogenesis. As expressed in the introduction the choice of VEGF as one of the variables was mainly due to our desire to include bevacizumab into the system. Even if the equations are ODEs we have taken into

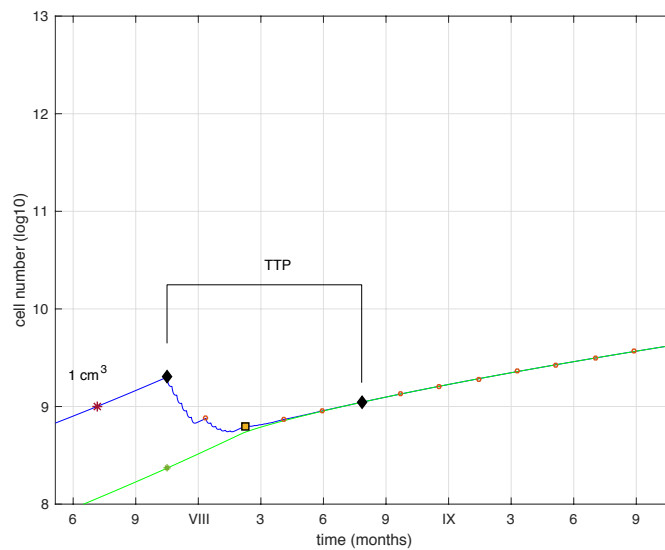
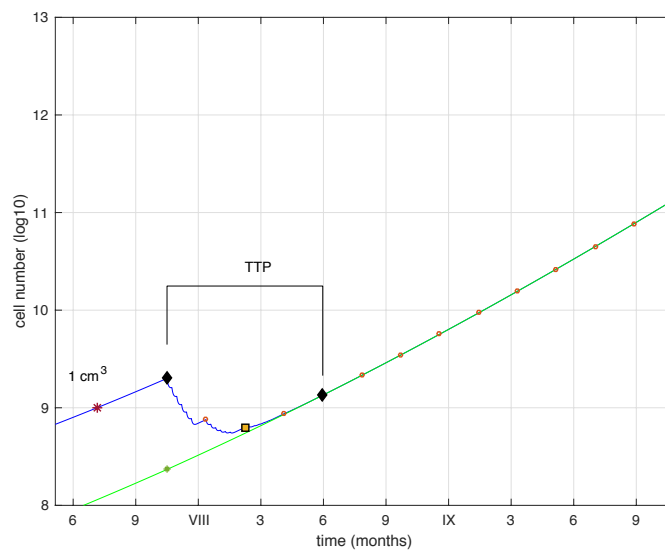


Figure 7: Zoom around treatment section. The first figure show the treatment with only 5-FU while the second with 5-FU plus BV5. Orange circles denote time of assessment of tumor size, the bigger square represents the nadir point and the two black diamonds denote the limits for TTP.

account the spatial structure through equations (1), (3), (5): the rule used here for the number of proliferating cells in absence of angiogenesis, namely $N_{boundary}^{norm}$, is a variant of Verhulst model, which has the form $N_t \left(1 - \left(\frac{N_t}{K}\right)^\alpha\right)$. We have devised this formula, based on geometrical considerations, to take into account the transition between an exponential growth and a slower growth when the number of cancerous cells is substantial. The 2/3 formula for VEGF was obtained from more physical argument, once more using the hypothesis of spherical symmetry. Due to the structure of the equations and their interaction we were able to obtain a curve of growth that results in a proper asymptotic rate in every phase of tumor development (figure 5).

Numerical simulations were used both as a validation mechanism for the model and as a way to obtain an estimate for some of the parameters. In order to extract more information from the simulations, comparison with clinical data was also performed: we focused on the specific case of colorectal cancer and measure TTP following the treatment prescribed in [29]. In this case we use TTP as an output to obtain additional informations on the parameters involved in the therapy.

The sets of parameters shown in table 1 is able to match all the quantitative key landmarks imposed in section 4.1, as well as TTP in both regimen 5FU and 5FU+BV5.

In a subsequent work we shall investigate the modifications played by the explicit introduction of metastases, their growth, size at the time when therapy starts, impact on TTP computation. Another generalization we have in mind, which moreover has been the initial motivation of our study, is to investigate more complex therapies, as those summarized in [12]. We have preferred to isolate the simplest case here because it may be modified to treat other types of cancer, due to its simplicity.

References

- [1] L. Arakelyan, Y. Merbl, P. Daugulis, Y. Ginosar, V. Vainstein, V. Selitser, Y. Kogan, H. Harpak, Z. Agur, Multi-Scale Analysis of Angiogenic Dynamics and Therapy, *Cancer Modelling and Simulation*, 2003.
- [2] Katerina D. Argyri, Dimitra D. Dionysiou, Fay D. Misichroni, Georgios S. Stamatakos, Numerical simulation of vascular tumour growth under antiangiogenic treatment: addressing the paradigm of single-agent bevacizumab therapy with the use of experimental data, *Biology Direct*, 2016, 11:12.
- [3] Agur, Z., Bloch, N., Gorelik, B., Kleiman, M., Kogan, Y., Sagi, Y., D. Sidransky, Ronen Y., Developing Oncology Drugs Using Virtual Patients of Vascular Tumor Diseases, *Systems Bio in Drug Discovery*, pp. 201-237.
- [4] S. Benzekry, Modélisation et analyse mathématique de thérapies anti-cancéreuses pour les cancers métastatiques, Ph.D. Thesis, Université de Provence, 2011.

- [5] S. Benzekry, D. Barbolosi, A. Benabdallah, F. Hubert, P. Hahnfeldt, Quantitative Analysis of the Tumor/Metastasis System and its Optimal Therapeutic Control, preprint.
- [6] S. Benzekry, G. Chapuisat, J. Ciccolini, A. Erlinger, F. Hubert, A new mathematical model for optimizing the combination between antiangiogenic and cytotoxic drugs in oncology, *C. R. Math. Acad. Sci. Paris* **350** (2012), n. 1-2, 23-28.
- [7] A. R. Bianco, S. De Placido, G. Tortora, *Core curriculum. Oncologia clinica*, McGraw-Hill 2011.
- [8] S. Bolin, E. Nilsson, R. Sjö Dahl, Carcinoma of the colon and rectum—growth rate, *Annals of surgery* **198** (1983), n. 2, 151-158.
- [9] A. Brù, S. Albertos, J. L. Subiza, J. L. Garcia-Asenjo, I. Brù, The universal dynamics of tumor growth, *Biophys. J.* **85** (2003), 2948-2961.
- [10] S. Chinnathambia, D. Velmuruganb, N. Hanagatad, Investigations on the interactions of 5-fluorouracil with bovine serum albumin: Optical spectroscopic and molecular modeling studies, *Journal of Luminescence* **151**, (2014), 1-10.
- [11] A. J. Coldman, J.M. Murray, Optimal control for a stochastic model of cancer chemotherapy, *Math. Biosciences* **168** (2000) 187-200.
- [12] C. Cremolini, M. Schirripa, C. Antoniotti, R. Moretto, L. Salvatore, G. Masi, A. Falcone, F. Loupakis, First-line chemotherapy for mCRC - a review and evidence-based algorithm, *Nature Reviews Clinical Oncology* **12** (2015), 607-619.
- [13] A D’Onofrio, A Gandolfi, A family of models of angiogenesis and anti-angiogenesis anti-cancer therapy, *Math. Medicine and Biology* **26** (2009), n.1, 63-95.
- [14] A D’Onofrio, A Gandolfi, Chemotherapy of vascularised tumours: role of vessel density and the effect of vascular "pruning", *J Theor Biol.*, 2010 May 21;264(2):253-65.
- [15] J. W. Drake, B. Charlesworth, D. Charlesworth, J. F. Crow, Rates of spontaneous mutation, *Genetics* **148** (1998), 1667-1686.
- [16] E.A. Eisenhauer, P. Therasse, J. Bogaerts, L.H. Schwartz, D. Sargent, R. Ford, J. Dancey, S. Arbuck, S. Gwyther, M. Mooney, L. Rubinstein, L. Shankar, L. Dodd, R. Kaplan, D. Lacombe, J. Verweij, New response evaluation criteria in solid tumours: Revised RECIST guideline, *European J. Cancer* **45** (2009), 228-247.
- [17] S. Friberg, S. Mattson, On the growth rates of human malignant tumors: implications for medical decision making, *Journal of Surgical Oncology* **65** (1997), 284-297.

- [18] Mac Gabhann F1, Popel AS, Targeting neuropilin-1 to inhibit VEGF signaling in cancer: Comparison of therapeutic approaches, *PLoS Comput Biol.*, 2006 Dec 29;2(12).
- [19] Z. Gao, M. J. Wyman, G. Sella, M. Przeworski, Interpreting the dependence of mutation rates on age and time, *PLOS Biology*, 2016, 1-16.
- [20] J. Gaudreault, G. Lieberman, F. Kabbinavar, V. Hsei, Pharmacokinetics (PK) of bevacizumab (BV) in colorectal cancer, *Clinical Pharmacology and Therapeutics* 69 (2001).
- [21] J. H. Goldie, A. J. Coldman, The genetic origin of drug resistance in neoplasms: implications for systemic therapy, *Cancer Research* 44 (1984), 3643-3653.
- [22] W. Grady, J. M. Carethers, Genomic and epigenetic instability in colorectal cancer pathogenesis, *Gastroenterology* 135 (2008), n. 4, 1079-1099-
- [23] P. Hahnfeldt, D. Panigrahy, J. Folkman, L. Hlatky, Tumor development under angiogenic signaling: a dynamical theory of tumor growth, treatment, response and postvascular dormancy, *Cancer Research* 59 (1999), 4770-4775.
- [24] P. Hinow, P. Gerlee, L. J. McCawley, V. Quaranta, M. Ciobanu, S. Wang, J. M. Graham, B. P. Ayati, J. Claridge, K. R. Swanson, M. Loveless, A. R. A. Anderson, A spatial model of tumor-host interaction: application of chemotherapy, *Math Biosci Eng.* 6 (2009), n. 3, 521-546.
- [25] G. Housman, S. Byler, S. Heerboth, K. Lapinska, M. Longacre, N. Snyder, S. Sarkar, Drug Resistance in Cancer: An Overview, *Cancers* 6 (2014), 1769-1792.
- [26] H. I. Hurwitz, L. Fehrenbacher, J. D. Hainsworth, W. Heim, J. Berlin, E. Holmgren, J. Hambleton, W. F. Novotny, F. Kabbinavar, Bevacizumab in combination with fluorouracil and leucovorin: an active regimen for first-line metastatic colorectal cancer, *J. Clin. Oncol.* 23 (2005), 3502-3508.
- [27] Jain HV1, Nr JE, Jackson TL., Quantification of endothelial cell-targeted anti-Bcl-2 therapy and its suppression of tumor growth and vascularization, *Mol Cancer Ther.*, 2009 Oct;8(10):2926-36.
- [28] F. F. Kabbinavar, H. I. Hurwitz, L. Fehrenbacher, N. J. Meropol, W. F. Novotny, G. Lieberman, S. Griffing, E. Bergsland, Phase II, randomized trial comparing bevacizumab plus fluorouracil (FU)/leucovorin (LV) with FU/LV alone in patients with metastatic colorectal cancer, *J. Clin. Oncol.* 21 (2003), 60-65.
- [29] F. F. Kabbinavar, J. Schulz, M. McCleod, T. Patel, J. T. Hamm, J. R. Hecht, R. Mass, B. Perrou, B. Nelson, W. F. Novotny, Addition of Bevacizumab to Bolus Fluorouracil and Leucovorin in First-Line Metastatic Colorectal Cancer: Results of a Randomized Phase II Trial, *J. Clinical Oncology* 23 (2005), n. 16, 3697-3705.

- [30] R. R. Kaldate, A. Haregewoin, C. E. Grier, S. A. Hamilton, H. L. McLeod, Modeling the 5-Fluorouracil Area Under the Curve Versus Dose Relationship to Develop a Pharmacokinetic Dosing Algorithm for Colorectal Cancer Patients Receiving FOLFOX6, *The Oncologist* 17 (2012), 296-302.
- [31] N. Komarova, Stochastic modeling of drug resistance in cancer, *J. Theoret. Biology* **239** (2006) 351-366.
- [32] Klamka J1, Maurer H, Swierniak A., Local controllability and optimal control for a model of combined anticancer therapy with control delays, *Math Biosci Eng.*, 2017 Feb 1;14(1):195-216.
- [33] Landry, J., J. P. Freyer, and R. M. Sutherland. "A model for the growth of multicellular spheroids." *Cell Proliferation* 15.6 (1982): 585-594.
- [34] U. Ledzewicz, H. Schattler, Analysis of optimal controls for a mathematical model of tumor anti-angiogenesis, *Optim. Control Appl. Meth.*, 2006; 00:116
- [35] N. Machida, T. Yoshino, N. Boku, S. Hironaka, Y. Onozawa, A. Fukutomi, K. Yamazaki, H. Yasui, K. Taku, M. Asaka, Impact of baseline sum of longest diameter in target lesions by RECIST on survival of patients with metastatic colorectal cancer, *Japanese Journal of Clinical Oncology* **38** (2008), n.10, 689-694.
- [36] D. Marmé, N. Fusenig Editors, *Tumor Angiogenesis*, Springer-Verlag Berlin 2008.
- [37] S. Motl, Bevacizumab in Combination Chemotherapy for Colorectal and Other Cancers, *American J. Health-System Pharmacy* **62** (2005), n.10, 1021-1032.
- [38] Monica Simeoni, Paolo Magni, Cristiano Cammia, Giuseppe De Nicolao, Valter Croci, Enrico Pesenti, Massimiliano Germani, Italo Poggese, Maurizio Rocchetti, Predictive pharmacokinetic-pharmacodynamic modeling of tumor growth kinetics in xenograft models after administration of anticancer agents. *Cancer Res.* 2004 Feb 1; 64(3): 10941101.
- [39] Stefanini MO, Qutub AA, Mac Gabhann F, Popel AS., Computational models of VEGF-associated angiogenic processes in cancer, *Math Med Biol.*, 2012 Mar;29(1):85-94.
- [40] B. Perthame, Some mathematical models of tumor growth, 2015.
- [41] G. J Peters, J. Lankeimal, R. M. Kok, P. Noordhuis, C. J. van Groeningen, C. L. van der Wilt, S. Meyer, H. M Pinedo, Prolonged retention of high concentrations of 5-fluorouracil in human and murine tumors as compared with plasma, *Cancer Chemother Pharmacol* **31** (1993), 269-276.

- [42] C. Riganti, E. Mini, S. Nobili, Editorial: Multidrug resistance in cancer: pharmacological strategies from basic research to clinical issues, *Front. Oncol.* 2015.
- [43] S. Sadahiro, T. Suzuki, K. Ishikawa, T. Nakamura, Y. Tanaka, K. Ishizu, S. Yasuda, H. Makuuchi, C. Murayama, Estimation of the time of pulmonary metastasis in colorectal cancer patients with isolated synchronous liver metastasis, *Japan J. Clin. Oncol.* **35** (2005), n.1, 18-22.
- [44] M. Simeoni, P. Magni, C. Cammia, G. De Nicolao, V. Croci, E. Pesenti, M. Germani, I. Poggesi, and M. Rocchetti. Predictive pharmacokinetic-pharmacodynamic modeling of tumor growth kinetics in xenograft models after administration of anticancer agents. *Cancer Res.*, 64 :1094–1101, Feb 2004.
- [45] G. G. Steel, *Growth kinetics of tumor*, Oxford: Clarendon Press, 1977.
- [46] A. Talkington, R. Durrett, Estimating tumor growth rates in vivo, *Bull. Math. Biology* **77** (2015), n. 10, 1934-1954.
- [47] P. Therasse, S. G. Arbuck, E. A. Eisenhauer, J. Wanders, R. S. Kaplan, L. Rubinstein, J. Verweij, M. Van Glabbeke, A. T. van Oosterom, M. C. Christian, S. G. Gwyther, New guidelines to evaluate the response to treatment in solid tumors, *J. National Cancer Institute* **92** (2000), n.3, 205-216.
- [48] T.D. Tlsty, B.H. Margolin, K. Lum, Differences in the rates of gene amplification in nontumorigenic and tumorigenic cell lines as measured by Luria–Delbruck fluctuation analysis, *Proc. Natl Acad. Sci. USA* **86** (1989), n. 23, 9441-9445.
- [49] N. Umetani, T. Masaki, T. Watanabe, S. Sasaki, K. Matsuda, T. Muto, Retrospective radiographic analysis of nonpedunculated colorectal carcinomas with special reference to tumor doubling time and morphological change, *The American Journal of Gastroenterology* **95** (2000), 1794–1799;
- [50] R. A. Weinberg, *The Biology of Cancer*, second edition, Garland Science, Taylor and Francis Group, New York 2014.
- [51] B. Zhao, S. M. Lee, H.-J. Lee, Y. Tan, J. Qi, T. Persigehl, D. P. Mozley, L. H. Schwartz, Variability in Assessing Treatment Response: Metastatic Colorectal Cancer as a Paradigm, *Clin Cancer Res*; **20** (2014), n. 13, 3560-3568.